Anal. Chem. **2010,** *82,* 5518–5526

Diamond, Titanium Dioxide, Titanium Silicon Oxide, and Barium Strontium Titanium Oxide Nanoparticles as Matrixes for Direct Matrix-Assisted Laser Desorption/Ionization Mass Spectrometry Analysis of Carbohydrates in Plant Tissues

Yousef Gholipour,[†] Silvana L. Giudicessi,[‡] Hiroshi Nonami,[†] and Rosa Erra-Balsells*[,‡]

Plant Biophysics/Biochemistry Research Laboratory, Faculty of Agriculture, Ehime University, 3-5-7 Tarumi, Matsuyama 790-8566, Japan, and CIHIDECAR-CONICET, Departamento de Química Orgánica, Facultad de Ciencias Exactas y Naturales, Universidad de Buenos Aires, Pabellón II, 3 P, Ciudad Universitaria, 1428-Buenos Aires, Argentina

Nanoparticles (NPs) of diamond, titanium dioxide, titanium silicon oxide, barium strontium titanium oxide, and silver (Ag) were examined for their potential as MALDI matrixes for direct laser desorption/ionization of carbohydrates, especially fructans, from plant tissue. Two sample preparation methods including solvent-assisted and solvent-free (dry) NPs deposition were performed and compared. All examined NPs except for Ag could desorb/ionize standard sucrose and fructans in positive and in negative ion mode. Ag NPs yielded good signals only for nonsalt-doped samples that were measured in the negative ion mode. In the case of in vivo studies, except for Ag, all NPs studied could desorb/ionize carbohydrates from tissue in both the positive and negative ion modes. Furthermore, compared to the results obtained with soluble sugars extracted from plant tissues, fructans with higher molecular weight intact molecular ions could be detected when the plant tissues were directly profiled. The limit of detection (LOD) of fructans and the ratios between signal intensities and fructan concentrations were analyzed. NPs had similar LODs for standard fructan triose (1-kestose) in the positive ion mode and better LODs in the negative ion mode when compared with the common crystalline organic MALDI matrixes used for carbohydrates (2,5-dihydroxybenzoic acid and nor-harmane) or carbon nanotubes. Solvent-free NP deposition on tissues partially improves the signal acquisition. Although lower signal-to-noise ratio sugar signals were acquired from the tissues when compared to the solvent-assisted method, the reproducibility averaged over all sample was more uniform.

In situ characterization of biomolecules using matrix-assisted laser desorption/ionization mass spectrometry (MALDI-MS) is a valuable biochemistry tool, provided that a suitable matrix capable of laser desorption/ionization (DI) of a given metabolite is available. In the case of neutral carbohydrates, which are the main plant metabolites, poor ionization in both ionic modes is a common difficulty in MALDI-MS analysis. Except in a few reports,[1,2] including those from our lab,[3,4] several crystalline organic matrixes, including 2,5-dihydroxybenzoic acid (DHB),[5−7] α-ciano-4-hydroxycinnamic acid (CHCA),[5−7] nor-harmane (9*H*-pyrido[3,4-*b*]indole; norHo),[5−8] and 2,4,6-trihydroxyacetophenone (THAP),[4−7] which are successful as the matrixes in MALDI-MS of carbohydrates, fail to cause DI of carbohydrates when the matrixes are deposited on the surface of plant tissues.[3,4] This failure may originate from the fact that when the matrixes are deposited on biological tissues and before the laser shooting, the matrixes incorporate into the tissue, which yields chemical interactions or linkages with tissue metabolites and structural components. These interactions and linkages diminish or suppress the signaling of the matrix and tissue.[4]

The presence of functional groups such as carboxylic and/or phenolic groups in DHB, CHCA, and THAP would cause strong tissue interactions. No such chemical interactions in the electronic ground state (before laser shooting) are theoretically expected in the potential MALDI matrixes when they are used for tissue analysis by deposition on the tissue. As long they have high absorption in the wavelength region of common MALDI-MS lasers

* To whom correspondence should be addressed. Phone/Fax: +54-11-45763346. E-mail: erra@qo.fcen.uba.ar.

[†] Ehime University.

[‡] Universidad de Buenos Aires.

(1) Stahl, B.; Linos, A.; Karas, M.; Hillenkamp, F.; Steup, M. *Anal. Biochem.* **1997**, *246*, 195–204.

(2) Robinson, S.; Warburton, K.; Seymour, M.; Clench, M.; Thomas, J. *New Phytol.* **2007**, *173*, 438–444.

(3) Gholipour, Y.; Nonami, H.; Erra-Balsells, R. *J. Am. Soc. Mass Spectrom.* **2008**, *19*, 1841–1848.

(4) Gholipour, Y.; Nonami, H.; Erra-Balsells, R. *Anal. Biochem.* **2008**, *383*, 159–167.

(5) Harvey, D. J. *Mass Spectrom. Rev.* **1999**, *18*, 349–451.

(6) Harvey, D. J. *Mass Spectrom. Rev.* **2006**, *25*, 595–662.

(7) Harvey, D. J. *Mass Spectrom. Rev.* **2008**, *27*, 125–201.

(8) Nonami, H.; Fukui, S.; Erra-Balsells, R. *J. Mass Spectrom.* **1997**, *32*, 287–296.

10.1021/ac1003129
Published on Web 06/02/2010

(337 and 355 nm),[9] inorganic nanoparticles (NPs) fulfill the above-mentioned condition and are potential candidates for direct molecular profiling of biological tissues. Furthermore, NPs have size-dependent physical and chemical properties that include their interaction with ultraviolet (UV) light.[9,10]

The use of NPs as the matrix for laser DI was considered in the early days of development of soft laser DI-MS. Tanaka et al.[11] used a fine powder (20-nm particles) of inorganic cobalt for protein and polymer analyses. Since then, especially in the past decade, several carbon-related NPs, including graphite[12] and carbon nanotubes (CNT)[13,14] and many metallic NPs such as TiO_2,[15,16] Ag,[17−20] silicon,[21] Au,[18,22,23] and zinc oxide,[24] have been examined for their potential use in MALDI and surface-ALDI-MS of organic molecules and biomolecules in both bare and capped forms. In addition, diamond NPs have been applied as a support for MALDI-MS targets to help increase the uniformity of the crystallization of the CHCA matrix.[25] The feasibility of using CNTs for direct plant tissue profiling to detect neutral carbohydrates in positive ion mode,[3,4] using colloidal graphite[26] for the detection of small metabolites from fruit tissues and using TiO_2 for the detection of triacylglycerols, flavonoids, and anthocyanines in plant tissues[16] have been recently reported.

In the present paper, we examined for the first time the capabilities of NPs of diamond, silver (Ag), titanium oxide (TiO_2), barium strontium titanium oxide (($BaTiO_3$) ($SrTiO_3$); BaSrTiO), and titanium silicon oxide ((SiO_2) (TiO_2); TiSiO) for in situ MALDI-MS analysis of carbohydrates in tissues from tulip and garlic bulbs. These tissues naturally contain soluble sugars, primarily sucrose and fructan oligosaccharides. The analyses were attempted in both positive and negative ion modes. Here, in addition to solvent-assisted transfer of NPs on tissues, we examined whether solvent-free deposition of NPs could improve direct MALDI-MS tissue analysis. The results were compared with those obtained after extraction of soluble carbohydrates from the bulb tissue, using the NPs as matrixes.

Select properties of the NPs that were related to the in vitro desorption/ionization of fructans were additionally explored. The limit of detection (LOD) and signal shot-to-shot reproducibility for 1-kestose (fructan triose; F3) deposited on the NPs matrixes were compared with those of crystalline matrixes including DHB and norHo as well as CNT matrixes. The ratio between the intensity (and relative intensity) of the carbohydrate signal and its solution concentration when NPs were used as matrixes was also studied.

MATERIALS AND METHODS

Materials. HPLC grade methanol (MeOH), ethanol (ETOH), chloroform ($CHCl_3$), and acetone (Merck, Darmstadt, Germany) were used without further purification. Nanopowders of diamond (≥97% purity, <10-nm size and BET surface area 278−335 m^2/g), TiSiO (99.8% purity, and <50-nm size), BaSrTiO (99.7% purity, <100-nm size), norHo, DHB, glucose, fructose (F1), and sucrose (F2) were purchased from Sigma-Aldrich Chemical Co., USA. Titanium dioxide (DP-25-nm diameter with ∼80% anatase and 20% rutile) was obtained from Evonik Degussa, Corp., USA. Silver NPs (<20 nm) suspended in water were obtained from British Biocell International. Multiwalled 10−30-nm carbon nanotubes; fructans, including 1-kestose (>99% purity; triose; F3), nystose (>99% purity; tetraose; F4), and 1^F-fructofuranosylnystose (>80% purity; pentaose; F5); and KCl were obtained from Wako Chemicals, Japan. Water with very low conductivity of Milli-Q grade that was purified at 56−59 nS/cm with a PURIC-S, (Orugano Co., Ltd., Tokyo, Japan) was used. Tulip (cultivar *Oxford*) and garlic bulbs were supplied by local growers.

Inorganic Nanoparticles. TiO_2 is commercially available as a nanopowder with a nominal particle diameter (25 nm) and specific surface area (55 $m^2\ g^{-1}$). It produced large aggregates during the drying process. The best results were obtained when the NPs were purified as follows:[27] TiO_2 (DP-25 TiO_2, Degussa) was thoroughly washed by dialysis until the conductivity of the supernatant solution was the same as that of water, then the product was vacuum-dried and stored in a dry atmosphere (desiccator) in the dark. Aggregates were then powdered by an agatha mortar and pestle. The BET specific surface area was determined from the N_2 adsorption isotherm at 77 K to be 51.4 $m^2\ g^{-1}$. The XRD pattern of the powder indicated that it is composed mainly of anatase (the content of rutile was less than 10%).

Different ways of suspending and applying the NPs onto the plate were tested. First, water was used for suspending particles, but this approach did not yield satisfactory results, and the signals intensities were extremely low. Among the different MeOH/H_2O mixtures tested, the 1:1 (v/v) was the best. NPs (50 mg) were added to 1 mL of a H_2O/MeOH (1:1) solution. Because the NPs sedimented quickly, it was necessary to resuspend by vortexing prior to their application on the sample probe or tissue. Ag NPs were applied in their original aqueous suspension form.

Organic Matrixes and CNTs. Solutions of DHB and norHo were prepared by dissolving 2 mg of matrix in 1 mL of a H_2O/

(9) Schmid, G. *Nanoparticules. From Theory to Applications*; Wiley-VCH Verlag GmbH & Co. KgaA: Weinheim, Germany, 2004.
(10) Watanabe, K.; Menzel, D.; Nilius, N.; Freud, H.-J. *Chem. Rev.* **2006**, *106*, 4301–4320.
(11) Tanaka, K.; Waki, H.; Ido, Y.; Akita, S.; Yoshida, Y.; Yoshida, T. *Rapid Commun. Mass Spectrom.* **1988**, *2*, 151–153.
(12) Sunner, J.; Dratz, E.; Chen, Y. C. *Anal. Chem.* **1995**, *67*, 4335–4342.
(13) Xu, S.; Li, Y.; Zou, H.; Qiu, J.; Guo, Z.; Guo, B. *Anal. Chem.* **2003**, *75*, 6191–6195.
(14) Pan, C.; Xu, S.; Hu, L.; Su, X.; Ou, J.; Zou, H.; Guo, Z.; Zhang, Y.; Guo, B. *J. Am. Soc. Mass Spectrom.* **2005**, *16*, 883–892.
(15) Lee, K. H.; Chiang, C. K.; Lin, Z. H.; Chang, H. T. *Rapid Commun. Mass Spectrom.* **2007**, *21*, 2023–2030.
(16) Lorkiewicz, P; Yappert, M. C. *Anal. Chem.* **2009**, *81*, 6596–6603.
(17) Sluszny, C.; Yeung, E. S.; Nikolau, B. J. *J. Am. Soc. Mass Spectrom.* **2005**, *16*, 107–115.
(18) Castellana, E. T.; Sherrod, S. D.; Russell, D. H. *JALA* **2008**, *13*, 330–334.
(19) Chiu, T. C.; Chang, L. C.; Chiang, C. K.; Chang, H. T. *J. Am. Soc. Mass Spectrom.* **2008**, *19*, 1343–1346.
(20) Shrivas, K.; Wu, H. F. *Rapid Commun. Mass Spectrom.* **2008**, *22*, 2863–2872.
(21) Wen, X.; Dagan, S.; Wysocki, V. H. *Anal. Chem.* **2007**, *79*, 434–444.
(22) McLean, J. A.; Stumpo, K. A.; Russell, D. H. *J. Am. Chem. Soc.* **2005**, *127*, 5304–5305.
(23) Su, C. L.; Tseng, W. L. *Anal. Chem.* **2007**, *79*, 1626–1633.
(24) Watanabe, T.; Kawasaki, H.; Yonezawa, T.; Arakawa, R. *J. Mass Spectrom.* **2008**, *43*, 1063–1071.
(25) Wei, L. M.; Xue, Y.; Zhou, X. W.; Jin, H.; Shi, Q.; Lu, H. J.; Yang, P. Y. *Talanta* **2008**, *74*, 1363–1370.
(26) Zhang, H.; Cha, S.; Yeung, E. S. *Anal. Chem.* **2007**, *79*, 6575–6584.
(27) Rodriguez, R.; Blesa, M. A.; Regazzoni, A. E. *J. Colloid Interface Sci.* **1996**, *177*, 122–131.

Table 1. Dynamic Range and LOD of 1-Kestose Using Different NPs in the Positive Ion Mode[a]

	without dopant		with KCl dopant		with NaCl dopant	
matrix	dynamic range	LOD	dynamic range	LOD	dynamic range	LOD
diamond	50−25 000	50	5−25 000	5	5−25 000	5
TiSiO	5−25 000	5	2.5−25 000	2.5	2.5−25 000	2.5
BaSrTiO	1.2−25 000	1.2	2.5−25 000	2.5	2.5−25 000	2.5
TiO_2	2.5−25 000	2.5	2.5−25 000	2.5	2.5−25 000	2.5
Ag[b]	ND		ND		ND	
CNTs	50−25 000	50	250−25 000	250	500−25 000	500
DHB	1.2−25 000	1.2	5−25 000	5	50−25 000	50
norHo	250−25 000	250	50−25 000	50	50−25 000	50

[a] Indicated as picomoles of 1-kestose deposited on the probe; S/N ≥ 6.5. [b] ND, no signal was detected.

Table 2. Dynamic Range and LOD of 1-Kestose Using Different NPs in the Negative Ion Mode[a]

	without dopant		with KCl dopant		with NaCl dopant	
matrix	dynamic range	LOD	dynamic range	LOD	dynamic range	LOD
diamond	250−25 000	250	500−25 000	500	500−25 000	500
TiSiO	50−25 000	50	5000−25 000	5000	50−25 000	50
BaSrTiO	50−25 000	50	50−25 000	50	500−25 000	500
TiO_2	50−25 000	50	500−25 000	500	500−25 000	500
Ag	50−25 000	50	500−25 000	5000	5000−25 000	5000
CNTs	250−25 000	250	5000−25 000	5000	5000−25 000	5000
DHB[b]	ND		ND		ND	
norHo	250−25 000	250	5000−25 000	5000	5000−25 000	5000

[a] Indicated as picomoles of 1-kestose deposited on the probe. S/N ≥ 13.5. [b] ND, no signal was detected.

MeOH (1:1) solution. CNTs were purified by successive rinsing and centrifuging with acetone and solutions of H_2O/MeOH ranging in ratios from 1:1 to 1:9. This process was followed by suspension in a H_2O/MeOH (1:9) solution as described elsewhere.[3,4]

MALDI-MS Analysis. All mass spectra were performed on a Voyager-DE STR time-of-flight mass spectrometer (Applied Biosystems, Foster City, CA) utilizing a 337-nm nitrogen laser with a 3-ns pulse width, delayed extraction in positive and negative ion modes and accelerating voltages of 20 kV. To obtain good resolution and signal-to noise (S/N) ratios, the laser power was adjusted to slightly above the threshold, and each mass spectrum was generated by averaging 100 lasers pulses per spot. Standard fructans were used for external calibration. Carbohydrate-related peaks detected by MALDI-MS of extracts and tissues were verified by comparison with those from standard fructans and maltoses as well as by the fragmentation patterns obtained by MS/MS analysis in post source decay (PSD) mode.

Sample Preparation. All soluble samples were spotted on a 100-well gold plate from Applied Biosystems. Matrix and sample applications were carried out using the dried-droplet method, in which 1.0 μL of the matrix solution is applied first and allowed to dry. Another 1.0 μL aliquot of the sample solution is then spotted on top of the matrix and air-dried.

In Vitro Analysis. Standard 25 mM solutions of sucrose (F2) and fructans (F3−F5) were prepared by dissolving the carbohydrate in a H_2O/MeOH (1:1) solution and in a H_2O/MeOH (1:1) solution with KCl (50 mM). Standard solutions with several carbohydrates in equimolar concentrations were prepared using the premix approach in which equal volumes of each standard sugar solutions were combined together and vortexed. The chemical 1-kestose, present in the studied tissues, was chosen for the determination and comparison of the experimental LODs that are achievable with DHB, norHo, CNTs, and the NPs studied herein. Serial dilutions of 1-kestose (25 mM) with H_2O/MeOH (1:1) were performed and analyzed. The lowest concentration tested was 1.2 μM. A 1.0-μL aliquot of each 1-kestose solution was spotted on a dry layer prepared with 1.0 μL of matrix solution (DHB or norHo), 1.0 μL of a CNT H_2O/MeOH (1:9) suspension, or 1.0 μL of a H_2O/MeOH (1:1) NP suspension. The LOD was defined as the number of picomoles of 1-kestose transferred on the probe that yielded a signal-to-noise ratio (S/N) that was greater than or equal to 6.5 in the positive ion mode and greater than or equal to 13.5 in the negative ion mode (see Tables 1 and 2). Each matrix was tested in both positive and negative modes. LOD experiments with 25 mM 1-kestose in H_2O/MeOH (1:1) with KCl (1 mM) that were successively diluted with H_2O/MeOH (1:1)−KCl (1 mM) were also conducted. Similar LOD experiments using 1-kestose in H_2O/MeOH (1:1) with NaOH (1 mM) diluted with H_2O/MeOH (1:1)−NaOH (1 mM) were also performed.

Soluble Carbohydrates Extracted from Tissues. For extracting the soluble carbohydrates from tulip bulbs or garlic bulbs, freeze-dried second scale from the bulbs stored at 5 °C for 9 weeks was homogenized with a mortar and pestle in a H_2O/EtOH (3:7) solution. After centrifuging at 3000*g* for 10 min, the soluble and insoluble phases were separated. The H_2O/EtOH soluble phase containing soluble carbohydrates was washed (extracted) with $CHCl_3$ to eliminate contaminants. Finally, it was passed through Waters Accell Plus QMA and Accell Plus CM cartridges for purification.

Tissue Preparation and Profiling. Slices (approximately 3 × 4 mm in size with less than 0.5-mm thickness) from the second scale of the tulip bulbs cultivar *Oxford* and from garlic bulbs after being stored under controlled temperatures (5, 17, and 25 °C) for 9 weeks were made by using a razor blade. Slices were

immediately placed on the MALDI plate without further preparation and air-dried.[4] Adhesive compounds for fixing the tissues on the plate were not used. The dried tissues were covered by 1.0 μL of NPs suspensions in solutions of H_2O/EtOH (1:1). They were air-dried again. For solvent-free (dry) deposition, NPs were homogeneously distributed on a polyethylene sheet and covered with tissues (freshly made and partially dried) for a few seconds, then the tissues were flipped and placed on the plate. Thus, dry NPs were uniformly distributed on the top of the tissue. In each experiment, three slices were examined, and 100 shots were recorded per slice. The accumulated mass spectra (consisting of 300 laser shots) are reported here. For each NP, an independent external calibration was carried out with mixed solutions of the five standard fructans (see above) deposited on an air-dried layer of the corresponding NP. Carbohydrate signals from the tissues were assigned by comparison with signals of standard carbohydrates observed in the linear and reflectron modes as well as with the fragmentation patterns obtained by MS/MS in the post source decay (PSD) mode.

RESULTS AND DISCUSSION

In Vitro Analysis of Fructans Using NPs: Limit of Detection Determination. To begin with our study of the application of NPs (diamond, TiO_2, TiSiO, BaSrTiO and Ag) as MALDI matrixes for direct tissue analysis of soluble carbohydrates (fructans), their behaviors as matrixes for commercially available fructans (fructose, F1; sucrose, F2; 1-kestose, F3; nystose, F4; and 1^F-fructofuranosylnystose; F5) were investigated (see structures of fructans in Figure S1 in the Supporting Information).

Carbohydrates that are soluble in cell sap are dissolved in aqueous solutions containing cations such as K^+ (50−100 mM) and Na^+ (5.0−5.5 mM) as well as Mg^{2+} and Ca^{2+} (<2.5 mM). Thus, soluble carbohydrates are detected in the MS positive ion mode mainly as potassiated species ($[M + K]^+$)[1,3−7] and in negative mode as deprotonated species ($[M - H]^-$) with either sucked cell sap[3] or direct cell/tissue MS analysis.[4,28] The results are quite different for native carbohydrate samples obtained after extraction. The content of Na^+ and the Na^+/K^+ ratio can change drastically due to the use of different aqueous solutions and chemicals during isolation, fractioning, and purification of the carbohydrates. Thus, in these samples, the content of Na^+ is higher than the content of K^+, which leads to the observation of mainly sodiated species $[M + Na]^+$ in the positive ion mode.[3−7]

Thus, to begin the in vitro MALDI-MS experiments, we used commercially available fructans in methanol aqueous solutions as well as methanol aqueous solutions doped with KCl or NaCl. As an example, in Figure 1, the spectra obtained in positive ion mode by deposition of KCl-doped equimolar solutions of fructans (F1, F2, F3, F4 and F5; 1:1:1:1:1 mol ratios; 500 μM of each in MeOH/H_2O (1:1) solution with 50 mM KCl) on air-dried layers of the examined NPs (diamond, TiSiO, BaSrTiO, and TiO_2) are shown. As can be seen, the efficiency of the desorption/ionization of each fructan as potassiated species as well as the

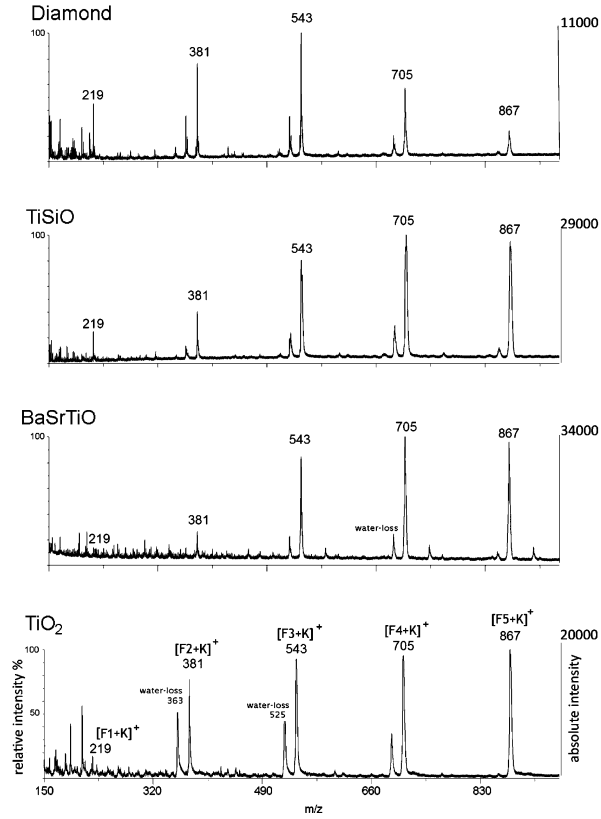

Figure 1. MALDI mass spectra of an equimolar mixture of commercial fructans (F1, F2, F3, F4, and F5; 500 uM in MeOH/H_2O (1:1)−KCl 50 mM) deposited on an air-dried layer of NPs (diamond, TiSiO, BaSrTiO, and TiO_2). Positive ion mode. Fructan ($[M + K]^+$ *m/z*): fructose, F1 (219); sucrose, F2 (381); 1-kestose, F3 (543), nystose, F4 (705), 1^F-fructofuranosylnystose: F5 (867).

clusters observed depend on the NP used. For example, diamond shows abundant polycarbon clusters in the region at $m/z < 200$ (see laser desorption ionization (LDI) mass spectra of all NPs used as matrix, DHB, norHo, and CNTs in Figure S2 in the Supporting Information). A similar conclusion was obtained from the negative ion mode experiments (see Figure S3 in the Supporting Information). Thus, LOD studies were conducted in both ion modes. Table 1 shows the comparison between the results obtained for 1-kestose deposited on the examined NPs (diamond, TiSiO, BaSrTiO, TiO_2, and Ag), on carbon nanotubes (CNTs) and on two crystalline organic matrixes currently used for carbohydrate analysis, DHB and norHo.

Experiments were conducted with KCl-doped 1-kestose solutions (prepared in H_2O/MeOH (1:1) with 1 mM KCl), NaCl-doped 1-kestose solutions (prepared in H_2O/MeOH (1:1) with 1 mM NaCl), and native 1-kestose (prepared in H_2O/MeOH (1:1)) solutions. The intensity of the monopotassiated ion $[M + K]^+$ (m/z 543) in the positive ion mode and $[M - H]^-$ (m/z 503) in the negative ion mode, were monitored in KCl-doped solutions. For NaCl-doped and nondoped fructan solutions, the species monitored were $[M + Na]^+$ (m/z 527) in the positive ion mode and $[M - H]^-$ (m/z 503) in the negative ion mode. The dynamic ranges in which fructan signal was detected with good signal/noise (S/N) ratios (S/N ≥ 6.5 in positive ion mode and S/N ≥ 13.5 in negative ion mode) and the respective LOD

(28) Yu, Z.; Chen, L. C.; Suzuki, H.; Ariyada, O.; Erra-Balsells, R.; Nonami, H.; Hiraoka, K. *J. Am. Soc. Mass Spectrom.* **2009**, *20*, 2304–2311.

Table 3. Dynamic Ranges[a] and Linearities ($0.99 > R^2 \geq 0.95$) of Standard Fructans Using Different NPs in the Positive Ion Mode[b]

NP	F2 (pmol)	F3 (pmol)	F4 (pmol)	F5 (pmol)
diamond		80−320	80−320	
TiSiO	20−1280	2.5−1280[c]	10−320	2.5−320
BaSrTiO	5−160	5−1280	20−320	20−320
TiO_2	20−1280	2.5−1280[c]	40−1280	20−1280

[a] Indicated as picomoles (pmol) of fructan deposited on the probe. [b] Sucrose, F2; 1-kestose, F3; nystose, F4; 1[f]-fructofuranosylnystose, F5. [c] $R^2 \geq 0.99$.

are listed in Tables 1 and 2. In the positive ion mode, all NPs except Ag showed comparably satisfactory LODs and dynamic ranges for 1-kestose. In the negative ion mode (Table 2), NPs were superior to DHB, norHo, and CNTs. Doping by KCl did not significantly improve the LOD in the positive ion mode (Table 1), and for all NPs except for BaSrTiO, there was a reduced LOD in the negative ion mode (Table 2). Results obtained for sucrose are included in Table S1 in the Supporting Information).

The examined NPs, except for Ag, have different dynamic ranges and linearities between the different concentrations of each fructan (F1−F5) and their $[M + Na]^+$ signal intensities ($m/z =$ 365, 527, 689, and 851, respectively) in the positive ion mode (Table 3). The results of examining the ratios of signal intensities to the concentrations of standard fructans deposited on NPs in positive ion mode showed a remarkable concentration sensitivity of the NPs, especially in the cases of TiSiO and TiO_2 (Table 3). This property was also evaluated as a ratio between the signal intensity of fructan 1-kestose (F3) and the signal intensity of the sucrose (F2) peak used as an internal standard (relative intensity). Solutions containing different concentrations of 1-kestose (10−1280 μM) in a solution of MeOH/H_2O (1:1) with 300 μM sucrose were used for these experiments (see Figures S4 and S5 in the Supporting Information). The plots presented in Figure S4 (positive ion mode) and Figure S5 (negative ion mode) exhibit good linearity when using TiSiO, BaSrTiO, and TiO_2 as matrixes in the positive ion mode and TiSiO and BaSrTiO in the negative ion mode. Results obtained for sucrose (F2) using 1-kestose (F3) as an internal standard and TiSiO and TiO_2 as matrixes are shown in the Supporting Information (Figure S6).

It is interesting to note that with increasing concentration of sugars deposited on the NPs (increasing the sugar concentration in the aqueous solution and the sugar to NP ratio; that is, 5 mM sugar solution), the DI efficiency decreased (the absolute intensity of the signal decreases instead of increases). Furthermore, the DI efficiency of the NPs was seen to be size-dependent because aggregation of the nanoparticles directly decreased the acquired signal, as well. NPs also showed different DI capabilities when using different solvents, including water and different water and methanol mixtures. This result suggests that solvent molecules attached on the surface of the NPs influenced surface-involved phenomena. The superiority of the NPs in the negative ion mode to common organic matrixes (DHB and norHo) probably originates from their higher capability to cause the surface-mediated deprotonation of sugars (see below).

TiO_2 (also known as titania) is the most widely used semiconductor photocatalyst.[29] Semiconductor photocatalysis is based on the following principles. After UV irradiation of a TiO_2 NP, the primary steps of the photoelectrochemical mechanism are as follows: (1) formation of charge carriers by a photon, (2) charge carrier recombination to liberate heat, (3) initiation of an oxidative pathway by a valence-band hole, (4) initiation of a reductive pathway by a conduction-band electron, (5) further thermal (i.e., hydrolysis or reaction with active oxygen species) and photocatalytic reactions to yield mineralization products, (6) trapping of a conduction-band electron in a dangling surficial bond to yield Ti(I1I), and (7) trapping of a valence-band hole at a surficial HO group.

The photochemical activity of titania is modified by promoting or suppressing the recombination of the electron pairs and hole pairs that are formed by UV light excitation. One of the methods to modify this property of titania is by the attachment of different metal oxides. The photoactivity of SiO_2-incorporated-titania is 3 times higher than that of TiO_2 Degussa P25.[30] However, the reasons why the photoactivity of silica-incorporated titania is higher than that of bare titania are not clearly understood.[31] It has been suggested that the reason might be related to the modification of the local environment of titanium surface species by the attachment of silica nanoparticles.

TiO_2 as a photocatalyst induces the oxidation and dimerization of alcohols,[32,33] and organic molecules, which include the HO functional group in their structure. This functional group is also included in carbohydrates structures. The photoinduced process is initiated by the loss of the H^+ unity from the alcohol, which can be followed by the capture of the electron ejected by TiO_2. The former step yields the $[M - H]^-$ species. Water molecules are selectively fixed on TiO_2 surfaces because of the interaction between Ti and the oxygen of water ($H_2O\cdots TiO_2$).[34,35] Thus, the amount of water present in the solvent of the NPs, in the analyte-tissue or in the prepared samples (analyte + NPs) for MALDI-MS analysis, can alter the capability of the NPs surface to interact with the analytes (carbohydrates). The aqueous methanol 1:1 (v:v) mixture used as the solvent in the present study showed better signals in both positive and negative ion modes.

$Ba_xSr_{1-x}TiO_3$ NPs, perovskite mixed-metal oxide crystals on the nanometer scale, have attracted sustained scientific and technological interest because of their ferroelectric properties and their very high surface−volume ratios.[36] Particularly, because the photocatalytic activity is related to the surface properties of these perovskites, powdered materials rather than single crystals or films were used.[36] Both BaSrTiO and TiSiO NPs as mixed-metal oxides retain

(29) Hoffmann, M. R.; Martin, S. T.; Choi, W. Y.; Bahnemann, D. W. *Chem. Rev.* **1995**, *95*, 69–96.
(30) Andreson, C.; Bard, A. J. *J. Phys. Chem.* **1995**, *99*, 9882–9885.
(31) Nur, H. *Mat. Sci. Eng. B* **2006**, *133*, 49–54.
(32) Muller, B. R.; Majoni, S.; Meissner, D.; Memming, R. *J. Photochem. Photobiol., A* **2002**, *151*, 253–265.
(33) Molinari, S.; Montocello, M.; Rezala, H.; Maldotti, A. *Photochem. Photobiol. Sci.* **2009**, *8*, 613–619.
(34) Blesa, M. A.; Morando, P. J.; Regazzoni, A. E. *Chemical Disolution of Metal Oxides*; CRC Press: Boca Raton, FL, 1994.
(35) Regazzoni, A. E.; Mandelbaum, P. A.; Matsusyoshi, M.; Shiller, S.; Bilmes, S. A.; Blesa, M. A. *Langmuir* **1998**, *14*, 868–874.
(36) Pena, M. A.; Fierro, J. L. G. *Chem. Rev.* **2001**, *101*, 1981–2018.

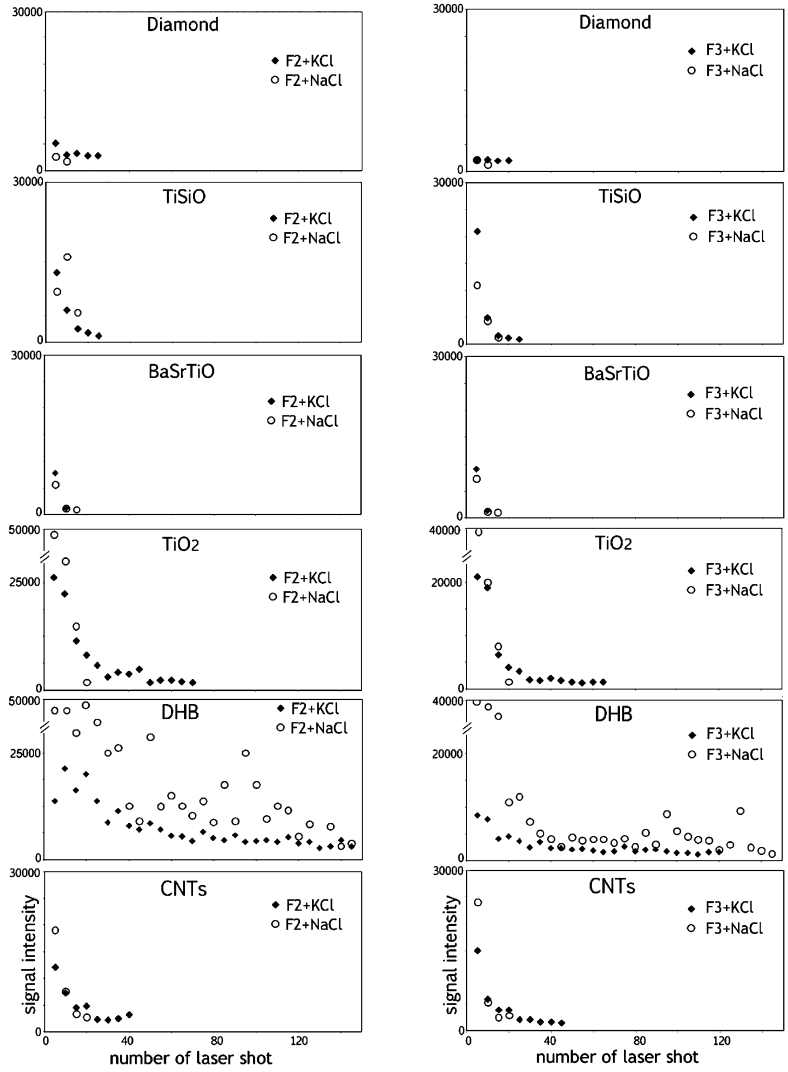

Figure 2. Capability of NPs to reproduce in vitro sucrose (F2; left panel) and 1- kestose (F3; right panel) signals compared with that of DHB and CNTs. All data were collected in the same position of a spot; each point represents the average intensity value of five laser shots on the fixed position on the plate. Signal intensity of *m/z* 365 $[F2 + Na]^+$, 381 $[F2 + K]^+$, 527 $[F3 + Na]^+$, and 543 $[F3 + K]^+$ were used. Solutions of fructan 80 μM in MeOH/H_2O (1:1)−KCl 50 mM and 80 μM in MeOH/H_2O (1:1)−NaCl 50 mM. Positive ion mode.

the photocatalytic properties of TiO_2. Thus, together with the partial ionization under laser irradiation, an important radiationless deactivation takes place that results in a significant increase in the local temperature. The heat is then transferred to the analyte molecules adsorbed on the particle surface, and they become well-desorbed/ionized. In positive ion mode, ionization is caused by adducts formation with K^+, Na^+, or both. In the negative ion mode, as was discussed above, because of the NP-induced deprotonation, the $[M - H]^-$ species was detected.

Diamond nanopowder with a mean particle size that is less than 10 nm has been described as a fluorescent nanomaterial.[37] Thus, it is expected that the efficiency of its radiationless deactivation is lower than those of nanopowders containing TiO_2.

NPs showed inferior signal shot-to-shot reproducibility compared to DHB (Figure 2). In the case of metal oxide NPs (TiSiO, BaSrTiO, and TiO_2) and CNTs, poorer signal reproducibility was accompanied by a sharp decrease in intensity and the very early disappearance of the signal of 1-kestose after consecutive laser shots. This outcome occurred despite the good desorption/ionization of the fructan after the primary shots (i.e., Figure 2 for TiSiO and TiO_2). In the case of diamond nanoparticles, however, a sharp decrease in intensity was not observed because low 1-kestose signal intensity was observed even for the starting laser shot. The partial radiative deactivation (fluorescence) of diamond NPs mentioned above would account for the minor DI induced in the carbohydrates. The enhanced photocatalyic behavior of BaSiTiO and TiSiO leads to lower shot-to-shot reproducibility compared with use of TiO_2. The above-mentioned photochemical oxidative catalytic properties of TiO_2, TiSiO and BaSrTiO NPs might be involved in this process and leads to the decomposition of fructans. Interestingly, as is also shown in Figure 2, NPs signal reproducibility was not affected by incorporating KCl or NaCl as a dopant.

(37) Boudou, J.-P.; Curmi, P. A.; Jelezko, F.; Wrachtrup, J.; Aubert, P.; Sennour, M.; Balasubramanian, G.; Reuter, R.; Thorel, A.; Gaffet, E. *Nanotechnology* **2009**, *20*, 235602.

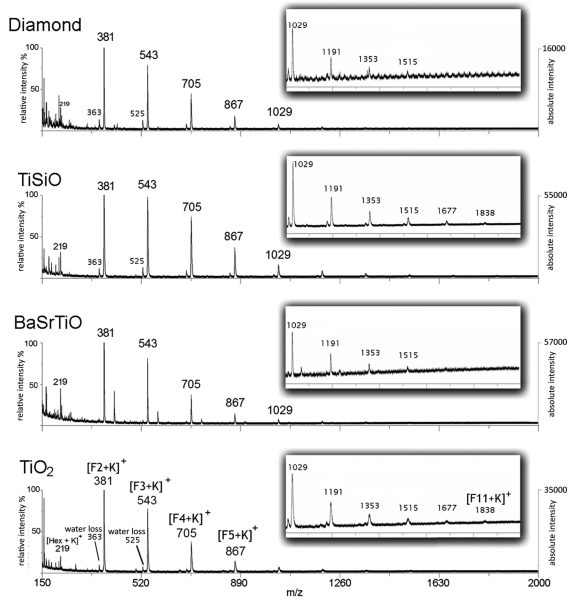

Figure 3. MALDI mass spectra acquired using NPs MeOH/H_2O (1:1) suspension deposited on tulip scale bulb tissue (bulbs stored at 5 °C); NPs: diamond, TiSiO, BaSrTiO, and TiO_2. Positive ion mode. Insets magnify the *m/z* 1000−2000 region.

In conclusion, the photochemical and physicochemical properties of NPs have a considerable effect on analyte DI processes, including thermal ablation processes.

Finally, it is interesting to note that although the reproducibility of the fructan signals in vitro is higher for DHB (Figure 2), this matrix does not successfully promote the desorption/ionization of fructans from tissue surfaces, as has been previously shown.[3,4]

Direct Profiling of Tissue: Solvent-Assisted Deposition of NPs. In positive ion mode, all NPs except Ag (results not shown) had signals corresponding to sucrose (*m/z* 381) and fructans as $[M + K]^+$ species originating from the surface of tulip tissues (Figure 3). The detected fructan *m/z* ranges were different when using different NPs. In general, diamond showed the smallest (Figure 3). Similar results were obtained from the surface of garlic tissues (see Figure S7 in the Supporting Information).

Compared to soluble fructan extracted from tulip bulbs (see Figure S8 in the Supporting Information), higher *m/z* signals of fructans were detected in these direct tissue profiling experiments (Figures 3 and Supporting Information S7). Higher relative abundances of the water-loss fragment signal were observed in these experiments and in those described in Figure 1. This outcome was probably caused by the fructan−NP surface interaction that induced (to some extent) the dehydration of the sugar. Furthermore, because the abundance of water loss signal of sugars varied with the nature of the NPs and the experiment (see the in vivo analyses, Figures 3 and Supporting Information S7, as compared with the in vitro analysis of Figures 1 and Supporting Information S8), we suggest that differences in the NP physical and chemical properties cause different interactions with the analyte molecules.

In the case of tissues, it is likely that a portion of the heat produced by UV-irradiated NPs is used to break hydrogen bonds between sugars and surrounding metabolites or tissue structures. Thus, the sugar molecules were less damaged and the quality of the acquired signal from tissue was quite good.

In the negative ion mode, the examined NP-yielded signals (except for Ag NPs) of deprotonated sucrose and fructans from the tissues. BaSrTiO NPs made the best matrix (see Figures S9 and S10 in the Supporting Information). Similar to the results described for positive ion mode analysis, the comparison of the NP MALDI-MS spectra of extracted soluble sugars with those of directly deposited NPs on tulip bulbs revealed that NP application directly on the tissue was successful in detecting fructans of high *m/z* in negative ion mode (see Figure S11 in the Supporting Information).

Finally, according to the literature,[38−40] low-temperature storage of tulip bulbs resulted in an increased content of fructans (especially those with low molecular weights), in sugar-storing cells of bulb scales. Direct profiling of tissues from tulip bulbs stored at 5 and 17 °C for 9 weeks by MALDI-MS using TiO_2 and the mixture (TiSiO + BaSrTiO) as matrixes enabled us to distinguish the tissues by their differing fructans contents (Figure 4). These results show that the method is suitably concentration-sensitive when applied for in situ quantitative tissue analyses.

Carbohydrate-related peaks detected by MALDI-MS of extracts and tissues were verified by comparison with those from standard fructans as well as by the fragmentation patterns obtained by MS/MS analysis in post-source decay (PSD) mode (see PSD MALDI-MS analysis for F2, F3, F4, and F5 in Figure S12 in the Supporting Information). It is interesting to note that monosaccharides such as glucose and fructose can be detected using the NPs here studied as MALDI matrixes (Figures S13 in the Supporting Information). Furthermore, glucose and fructose show different fragmentation pattern in PSD MALDI-MS experiments (see Figures S14 in the Supporting Information).

Direct Profiling of Tissue: Solvent-Free Deposition of NPs. The results obtained in positive ion mode using solvent-assisted and solvent-free deposition of NPs on tulip bulb tissue were not the same. As is shown in Figure 5, in positive ion mode, TiSiO failed as a matrix, whereas BaSrTiO NPs produced higher amounts of interfering signals. Furthermore, the relative intensity of fructan signals was lower. However, use of diamond NPs and mixtures of NPs did improve the signal acquisition and resolution in the solvent-free method (Figure 5, diamond + TiSiO and TiSiO + BaSrTiO). The lower chemical and photochemical reactivity of the diamond NP surface accounts for the observed results. Furthermore, in the negative ion mode, solvent-free deposition of NPs yielded sugar signals with S/N ratios similar to those obtained by NPs that underwent solvent-assisted deposition (see Figures S14 in the Supporting Information).

Finally, as shown in Figure 6, a morphological surface tulip bulb tissue inspection (digital image obtained by a Keyence digital microscope VHX-900 in scanning mode) showed that in general, a more uniform distribution of NPs was achieved when the solvent-assisted transferring method using fresh, gently vortexed NPs suspensions (Figure 6B) was applied; however, with this method, solvent movement and convectional movements inside the droplet on the tissue might cause some irregularities in the distribution of the NPs. Attention must be

(38) Moe, R.; Wickström, A. *Physiol. Plant.* **1973**, *28*, 81–87.
(39) Haaland, E.; Wickström, A. *Acta Hortic.* **1975**, *47*, 371–376.
(40) Lambrechts, H.; Rook, F.; Kolloffell, C. *Plant Physiol.* **1994**, *10*, 515–520.

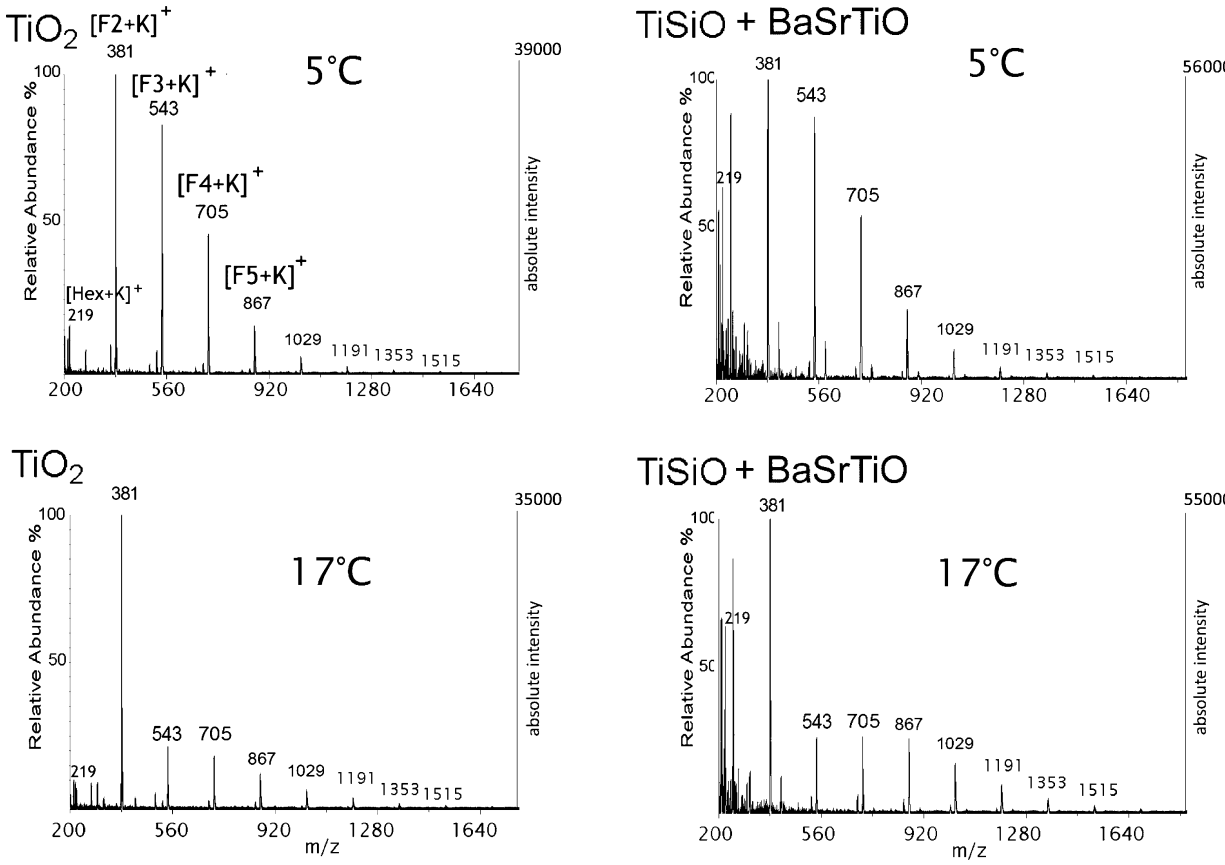

Figure 4. MALDI mass spectra acquired using NP MeOH/H_2O (1:1) suspension deposited on tulip scale bulb tissue (bulbs stored at 5 and 17 °C); NPs: TiO_2 and TiSiO + BaSrTiO (1:1); positive ion mode.

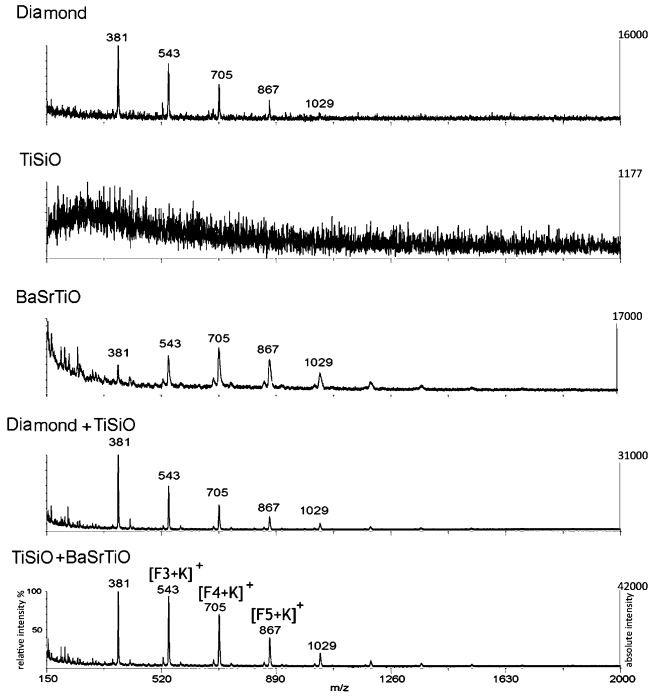

Figure 5. MALDI mass spectra acquired using dry NPs deposited on tulip scale bulb tissue (bulbs stored at 5 °C); NPs: diamond, TiSiO, BaSrTiO, diamond + TiSiO, TiSiO + BaSrTiO; positive ion mode.

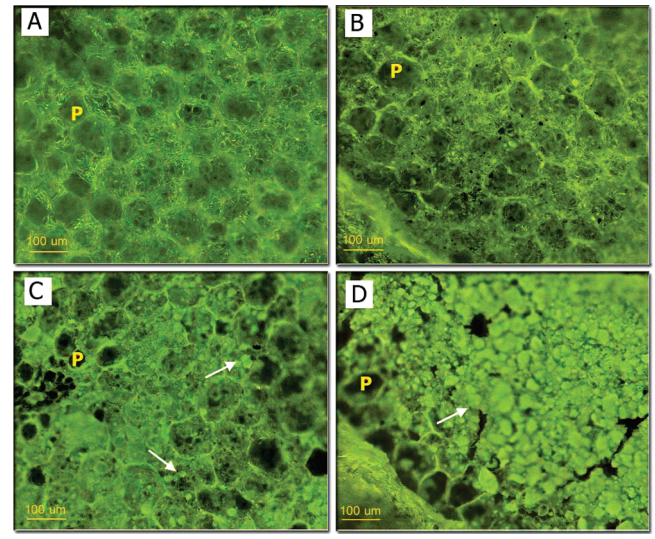

Figure 6. Morphological inspection of tulip bulb tissue samples: (A) tissue alone, P indicates sugar-storing parenchyma cells; (B) tissue covered by NPs of BaSrTiO deposited by using a fresh MeOH/H_2O (1:1) suspension, after gently vortexed; (C) tissue covered by NPs of BaSrTiO deposited by solvent-free deposition method; arrows point out big aggregates of NPs that are normally found in an original package of dry NPs; (D) old and poorly vortexed suspension of BaSrTiO in MeOH/H_2O (1:1) was used, arrow points out strong aggregation of NPs.

paid to any potential aggregation because large aggregates of NPs found in the original dry commercial packages decrease the uniformity of the NPs distributions on tissue surfaces. These aggregates should be removed prior to the experimenta-

tion (Figure 6C). In addition, when NPs from old or poorly vortexed suspensions were deposited on tissues using solvent-assisted transference, NP aggregation resulted in the formation of a shell-like structure (Figure 6D), which suppressed signals from both the matrix and the tissue.

CONCLUSIONS

Diamond, TiO_2, TiSiO, BaSrTiO NPs, and their mixtures can be useful for profiling tissues by MALDI-MS to determine the content of neutral carbohydrates. We have shown that potential chemical interactions with the NPs in the ground state and in the electronic excited state make the NPs potential matrixes for LDI of neutral carbohydrates from tissues. However, in practice, different NPs had different amounts of LDI capability related to their size (active surface area), composition, structure, and chemical and photochemical properties. We further concluded that their LDI capabilities might be affected by their surface−solvent or surface−tissue interactions. Additionally, the presence of a suitable physical linkage between the nanoparticles and the metabolites (neutral carbohydrates in this study) seemed to critically influence the LDI capabilities of the NPs. In solvent-free deposition of NPs, tissues in different states of dryness had different signal yields, suggesting that the relative abundance of water molecules directly affects the LDI properties of the NPs by connecting the NPs to the tissue or linking the NPs to the metabolites. We speculated that the surface attachment of the nanoparticles, in both bare and off-type molecules (i.e., molecules from solvent) is actively involved in the desorption/ionization processes and deserves further investigation in the hope that such study can provide insight regarding the events that occur during MALDI.

Higher molecular weight oligosaccharides were detected when the tissues were directly analyzed than when extracted carbohydrates from the same tissue were deposited on the NPs. This is an interesting aspect for UV−MALDI-MS application in vivo, in plant tissues, using the studied NPs as matrixes. This detection of higher molecular weight carbohydrates from tissues may be related to abundant in situ water molecules and cations, especially potassium, which results in a very soft ionization that consequently aids in the stability of the sugar molecules during MALDI-MS.

Finally, it is interesting to note that the concentrations of soluble carbohydrates in fresh plant tissues range from 0.1 to 1 M[41,42] (i.e., sweet grapes, soluble sugar concentration ~1 M; leaves and stems, soluble sugar concentration 0.1 − 0.2 M). Thus, the LODs reported in the present study are sufficient to analyze soluble carbohydrates in fresh plant tissues.

(41) Nonami, H.; Boyer, J. S. *Plant Physiol.* **1993**, *102*, 13–19.
(42) Boyer, J. S. Measuring the Water Status of Plants and Soils Pressure Probe, Academic Press: San Diego, 1995; Chapter 4.

ACKNOWLEDGMENT

This work was financially supported by Grant-in-Aid (S) from the Japan Society for the Promotion of Science (JSPS) for Scientific Research (20228004), UBA (X072), CONICET (PIP 00400), and ANPCyT (PICT 06-0615). R.E.-B. is a research member of CONICET. UV−MALDI-TOF MS was performed as part of the Academic Agreement between Rosa Erra-Balsells (FCEN-UBA, Argentina) and Hiroshi Nonami (CA-EU, Japan) with the High Resolution Liquid Chromatography-integrated Mass Spectrometer System of the United Graduated School of Agricultural Sciences (Ehime University, Japan) facility.

SUPPORTING INFORMATION AVAILABLE

Fifteen additional figures and one table are available in the Supporting Information. This material is available free of charge via the Internet at http://pubs.acs.org

Received for review February 4, 2010. Accepted May 21, 2010.

AC1003129